I

PAPER I

DISPERSION MEASUREMENTS USED IN SPECIAL CORE ANALYSIS OF CARBONATES

DISPERSION MEASUREMENTS USED IN SPECIAL CORE ANALYSIS OF CARBONATES

Arne Skauge, Bartek Vik, Shahram Pourmohammadi, and Kristine Spildo
Centre for Integrated Petroleum Research (CIPR),
University of Bergen, Norway

This paper was prepared for presentation at the International Symposium of the Society of Core Analysts held in Trondheim, Norway, 12-16 September 2006

ABSTRACT

Carbonate reservoirs are usually very heterogeneous and contain a wide range of different pore classes. The main pore classes are primary and secondary interparticle porosities, moldic porosity, vuggy porosity, intercrystalline porosity, chalk and chalky microporosity. Carbonate material may also contain pore structures like; vugs, molds, and fractures in addition to matrix pore-structure.

Single phase dispersion has been measured by injecting a slug of water tracer (Fluorinated Benzoic Acid) into carbonate rocks representative of different carbonate pore classes. The dispersion measurements have been interpreted by analysis of the convection-dispersion equation. We have used the capacitance model developed by Coats and Smith, which is a more elaborate and detailed approach than the standard convection-dispersion equation. Simulation of tracer production profiles quantifies dispersion coefficients, flowing fraction, dead-end pore fraction and inaccessible pore volumes.

Different carbonate pore classes show a large variation in fluid flow properties. The observations from dispersion analysis based on single phase flow are consistent with two-phase flow results. Large amounts of inaccessible and dead-end pores, which are poorly connected to the flowing-fraction of the pore-structure, are correlated with low oil recovery.

INTRODUCTION

Depending on the scale of the heterogeneity, dispersion in porous media has been studied in three main categories; microscopic (pore scale), macroscopic (core scale) and megascopic dispersion (field scale). The total microscopic dispersion in a porous medium is due to both molecular diffusion and convective mixing. Convective mixing in porous media is as a result of incomplete connectivity, with obstructions caused by local regions of reduced pressure, Aveyard and Haydon. The level of dispersion by this mechanism is suggested to be proportional to the flow velocity, Ewing. Dispersion can also be due to dead-end pores and adsorption as described by Coats and Smith. At the reservoir scale, however, dispersion is due to large scale heterogeneities such as stratification, shales,

blocks of variable permeability etc. Arya et al. have shown that macroscopic dispersivity is sensitive to diffusion in both laboratory and field scale. They have also concluded that macroscopic dispersivity is less or equal to megascopic dispersivity. At the field scale, dispersivity is grown by extension of the system compared to the laboratory scale, Arya et al.

Dispersion measurements have been done in both single and two-phase flow by tracer injection at both laboratory and field scale, and has already been applied in water reservoirs to study communication between wells (Hagoort, Salter and Mohanty, Smith, and Schwartz). Perkins and Johnson have investigated the effect of porous media properties such as particle to column-diameter ratio, particle size distribution and particle form on dispersion. Three different models for single-phase dispersion in porous media have been proposed (Coats and Smith, Deans) the standard diffusion model, the capacitance model and the differential capacitance model. Deans proposed a capacitance model to analyse asymmetrical effluent profiles observed by tracer injection into porous medium. In his model, three parameters mainly describe dispersion in the porous media; the number of stages, stagnant volume and mass transfer constant. The latter describes mass transfer between stagnant volume and flowing stream. Coats and Smith expanded the Deans model and showed an improved fit to experimental data. The Coats and Smith model is introduced by two equations:

$$D\frac{\partial^2 c}{\partial x^2} - v\frac{\partial c}{\partial x} = f\frac{\partial c}{\partial t} + (1-f)\frac{\partial c^*}{\partial t} \tag{1}$$

$$(1-f)\frac{\partial c^*}{\partial t} = M(c - c^*) \tag{2}$$

The first equation is derived from material balance whereas the second equation describes mass transfer between the stagnant volume and the flowing stream. The solution of Eq.1 is found in Coats and Smith. By using Eq.1, the fraction of dead-end pores (1-f), dispersion coefficient (D) and mass transfer constant (M) can be determined from tracer analysis. Tailing or capacitance of effluent concentration is related to dead-end pores. Fatt et.al (1966) estimated dead-end pore volume by a method based on applying resistivity measurements. Bingham showed that for both standard diffusion and differential-capacitance model, different boundary conditions give almost the same solution. Jasti et al. investigated the dependency of parameters defined in the Coats-Smith model on interstitial velocity. It was revealed that the mass-transfer coefficient between two regions is independent on interstitial velocity but is related to the geometry of the stagnant volume. Their experiments confirmed that tracer tailing is a function of the ratio of the molecular diffusivity to the flow rate.

In this study, an attempt was made to select carbonate materials that are representative of different carbonate pore classes. Porosity classification systems have been widely used to characterize carbonate reservoirs by petrophysicists and petroleum geologists. Among pore classification approaches, the ones developed by Choqutte and Pray, Archie and Lucia are

well known. The classification developed by Choqutte and Pray is linked to sedimentological fabric and difficult to correlate to flow units and flow properties. Pore system classifications by Archie and Lucia are preferred with respect to integration with dynamic models because they are easily linked to flow properties. On the other hand it is difficult to incorporate them into sedimentological modelling and they are also difficult to use in exploration. Lonoy recently proposed a new pore-system classification based on pore type, thin section analysis and porosity-permeability relations. According to this classification, carbonates can be divided into 20 pore classes. In this scheme, carbonates are divided into 6 main pore classes and then, based on the pore sizes, into two or three subdivisions. Patchy distribution of pores is due to selective dissolution or partially cementation of initially preserved pores, Lonoy.

Hashemi et al. used the Coats and Smith model to determine accessible pore volume analysed from miscible displacement. Fourar et al. have compared local flux and local concentration for carbonate cores by in-situ measurement of tracer concentration. It was observed that the dispersion coefficient is not constant along a core, and that there is a link between the porosity distribution and tracer dispersion.

EXPERIMENTAL

Material Selection

Carbonate core plugs were selected from four different basins and classified based on dominating pore classes as defined by Lonoy. Basic data, including pore class, for the selected core plugs are listed in Table 1. Vuggy carbonate cores used in this study are believed to be well connected and characterized as touching-vug pore class based on a Lucia-type of classification. Several intercrystalline pore types were studied to investigate the effect of pore size distribution and pore size on dispersion. However, IC-UMe and IC-PMa pore types were not included because they were not available. CT scan images for all selected core plugs were examined ensuring that there were no fractures within the core plugs. This was done to avoid the presence of micro-fractures which may dominate the dispersion behaviour.

Experimental Procedures

After cleaning by standard procedures, core plugs were saturated with brine to measure permeability and porosity. Perfluoro-Benzoic Acid was added to brine as the tracer, and slugs of 2 or 3 pore volumes tracer were injected into cores. The effluents were subsequently collected and analyzed by UV spectroscopy. After analyzing collected effluents, tracer concentrations versus injected pore volume of tracer were plotted. Tracer injection rates for the different core plugs are found in Table 1. After tracer tests, core plugs were flooded by lab oil to irreducible water saturation followed by a brine flood to residual oil saturation. The final recovery by water flooding is found in Table 1. Core plugs were believed to be water wet since they were initially cleaned and no restoration was made.

Analysis of Data by Simulation

The Coats and Smith model (1963) was used to analyze trace effluent profiles in this study. The UTCHEM simulator code 9.82 (UTCHEM-9.82, 2000) was used to simulate tracer injection into one dimension of a Cartesian system that was specified to have 100 grid cells. One injection and one production well were considered. Three main assumptions were made during the simulation steps; transversal dispersion is negligible, the mass transfer coefficient between stagnant volumes and flowing stream is constant and value of 0.0005 [S^{-1}] was used. Molecular diffusion was also assumed to be insignificant with respect to mass transfer and was thus ignored. Effluent profiles resulting from tracer experiments are in homogeneous and ideal cases symmetrical with almost 50% of the injected tracer concentration produced after one pore volume of tracer injection.

In heterogeneous porous media, dead-end pores lead to tailing (capacitance effect) due to mass transfer between fluids within dead-end pores and flowing stream. Inaccessible pores lead to earlier tracer breakthrough. Asymmetric tracer profiles reflect the effect of both inaccessible and dead-end pores. The slope of effluent the profiles are related to the degree of dispersivity. Two parameters were considered to obtain the best match with experimental data; flowing fraction (f) and dispersivity (α). Depending on the tailing (capacitance) observed in effluent profiles, the flowing fraction and dispersivity were tuned to obtain a satisfactory match between simulation and experimental data. After that, an attempt was made to match the point of breakthrough of 50% of the injected concentration by reducing the total porosity. Equations relating total porosity to inaccessible porosity, dead-end porosity and flowing porosity are found in the appendix.

RESULTS AND DISCUSSION

Experimental results were analyzed to characterize dispersion by single phase flow for selected carbonate core plugs. Further, the experiments were simulated with a capacitance model to estimate dispersivity, fraction of dead-end and inaccessible pores. The results are summarized in the Table 2 and Figures 1 to 12. Four main carbonate pore classes were analyzed. Results from the individual classes are discussed below.

Intercrystalline Pore Types

Figures 1 to 4 show results from tracer experiments on cores from the intercrystalline pore class. As the name implies, porous media belonging to this pore class are characterized by pores formed between crystals. The pores may be either primary or secondary in origin (Choquette and Pray). Secondary pore types are usually formed due to calcite recrystallization or dolomitization, and pore size distribution is controlled by patchy cementation (Lønøy).

As can be seen from Figures 1 and 4, the IC-UMa and IC-PMe pore types show clearly different responses by water tracer injection. Effluent profiles in Figure 1 for the IC-UMa pore types are representative of pore systems dominated by higher fraction of inaccessible

pores and less capacitance effects. The IC-PMe pore types in Figure 4, on the other hand, show a low fraction of inaccessible pores and more tailing due to a higher fraction of dead-end pores. Earlier breakthrough in effluents for the IC-UMa pore types are not due to higher permeability since intercrystalline uniform systems are believed to be less permeable than intercrystalline patchy pore types (Lønøy). The differential capacitance model used to analyze tracer effluent profiles confirms this hypothesis. The average inaccessible and dead-end porosity for the IC-UMa pore types are higher and lower respectively than for the IC-PMe pore types (Table 2 and Figure 12). Figure 12 also shows that the average flowing porosity, and recovery, is lower for for the IC-UMa pore types than for the IC-PMe pore types. It seems that a decrease in pore size for intercrystalline patchy pore types (IC-PMi) decreases the flowing porosity slightly (Figure 3 and Figure 12), while slightly increasing the amount of accessible pores, leading to lower recovery. For the IC-UMi pore types, it is hard to determine the effect of pore size because there is not enough data. The data also proved difficult to analyze using the capacitance model (see Figure 2). Among the IC-UMa pore types, core sample F48 has the lowest fraction of dead-end and inaccessible pores while F3 has the highest. This agrees well with the observation that recovery by waterflooding is highest for core F48 and lowest for core F3.

Moldic- Micro Pore Type

Cores belonging to the moldic micro pore type are expected to have either a low or a high fraction of inaccessible pores. Only two samples representative of this pore type were available, and Figure 5 shows their experimental tracer profiles. The profiles could be well described by the capacitance model, and a significantly higher dispersivity and fraction of dead-end pores was found for core plug F25 as compared to plug O3. Core plug F25 had a higher flowing fraction and thus oil recovery by waterflood. In order to have an idea of typical fractions of dead-end and inaccessible pores for this pore class more samples have to be analyzed.

Vuggy Pore Types

Lucia considered the vuggy and moldic pore types to belong to the same pore class. Choqutte and Pray, on the other hand, distinguished between them. Lønøy also distinguished between these two pore classes. Both vuggy and moldic pore types are formed by selective dissolutions of rock fabric at different scales (Lucia). The high permeability of vuggy core plugs used in this study indicates that vugs may be connected. Figure 6 shows effluent profiles measured for four samples. Among these plugs, core plug P4 has a different response to tracer injection compared to the others. This core plug has the lowest permeability and earliest breakthrough of injected tracer, as well as the lowest dispersivity and oil recovery by waterflooding.

The differential capacitance model indicates that this pore type has the highest fraction of inaccessible pores (see Table 2). Figure 13 shows that the average dead-end porosity is lower than the average fraction of inaccessible porosity for this pore type. Results from analyzing the tracer experiments using the differential capacitance model are in good agreement with the observed recovery. The low dispersivity of this material indicates that

it has a high connectivity. Core plug P4 has the lowest flowing fraction porosity as well as lowest oil recovery by waterflooding.

Chalky Micro Pore Types

Tracer effluent profiles of this pore class (Figure 7) indicate a negligible amount of inaccessible pores, and a low to significant fraction of dead-end pores. Although two of the tracer profiles could not be analyzed using the capacitance model, the two others show a low fraction of inaccessible pores (see Table 2). Nevertheless, recovery is high in these low permeable materials by water flooding.

Comparison of Measured and Modeled Dispersion for Characterization of Carbonate Pore System

The capacitance model used to evaluate dispersion in the studied carbonates materials lead us to divide them into four main groups regardless of their pore classes:

1. Carbonate materials with dispersion characteristics that can successfully be interpreted by the capacitance model to predict fractions of dead-end pores and inaccessible pores. Figure 8 shows effluent profiles from tracer injection experiments together with corresponding simulated results. It can be inferred that dispersion is controlled by dead-end and inaccessible pores for these materials.
2. Carbonate materials whose tracer profiles are stepwise and thus cannot be described by the capacitance model. Figure 9 shows three examples of this behaviour from three different pore classes.
3. Carbonates from which less than 0.5 of the injected water tracer is produced after one pore volume of injection (Figure 10). Material balance confirms that tracer is not absorbed inside the material.
4. Core materials with effluent profiles that are not S-shaped so that the capacitance model cannot be used to analyze and characterize dispersion. Figure 11 shows two examples of such responses. These materials should be further characterized by CT-scan to observe pore structures.

CONCLUSIONS

The capacitance model proposed by Coats and Smith can be used to describe single phase dispersion for a majority of different carbonate pore classes. This makes it possible to quantify the fraction of dead-end and inaccessible pores.

Complex dual-porosity pore classes like the moldic pore type may have good connectivity as indicated by the high flowing fraction inferred from the dispersion measurements.

Waterflood oil recovery is correlated to flowing fraction for almost all studied pore classes and the more fraction of flowing pores, higher recovery is expected.

Comparison of dispersion from tracer test with those predicted from Coats and Smith may be used to classify pore types. This classification should be a component of core characterization for SCAL of carbonates.

NOMENCLATURE

C=Concentration in produced fluid, mol/cm^2
C_0=Injected Concentration, mol/cm^2
C^*Average Concentration in Stagnant Volume or Dead-end Pores, mol/cm^2
D=Dispersion Coefficient, cm^2/s
f=Flowing fraction
K=Absolute Permeability, mD
M=Mass transfer constant between stagnant and flowing volumes, cm^2/s
PV=Pore Volume
v=Interstice velocity, cm/s
t=time's.
x=Dimension of flow, cm

Subscripts
CM=Capacitance Model
I=Inaccessible
D=Dead-End Pores
T=Total Porosity
Greek Letters:
α=Dispersivity, cm
Φ=porosity, fraction

Pore Type Codes:
IC-UMa= Intercrystalline, Uniform Macropores
IC-UMi= Intercrystalline, Uniform Micropores
M-Mi= Moldic Micropores
IC-PMe= Intercrystalline, Patchy Mesopores
IC-PMi= Intercrystalline, Patchy Micropores

ACKNOWLEDGEMENT

The authors would like to acknowledge support from Norsk Hydro.

REFERENCES

Archie, G.E., "Classification of Carbonate Reservoir Rocks and Petrophysical Considerations", AAPG Bulletin, (1952), v. 36, no. 2, p. 278-298.

Arya, A., Hewett, T.A., Larson, R.G., and Lake, L.W. ," Dispersion and Reservoir Heterogeneity", SPE Reservoir Eng. , (Feb. 1988) 139-148.

Aveyard,R. and Haydon,D.A: "An Introduction to the Principles of Surface Chemistry",Cambridge University Press, (1973) London.

Bringham, W.E.:"Mixing Equations in Short Laboratory Cores," SPEJ (Feb. 1974) 91-99, Trans., AIME, 257

Choquette, P. W., and L. C. Pray, "Geologic Nomenclature and Classification of Porosity in Sedimentary Carbonates" AAPG Bulletin, (1970), v. 54, no. 2, p. 207-250.

Coats, K.H. and Smith, B.D.:"Dead-End Pore Volume and Dispersion in porous Media," Trans.,AIME(1963) 231,73-84

Deans, H.A.:"A Mathematical Model for Dispersion in the Direction of Flow in Porous Media," AIME (1963) Vol. 228,49.

Ewing,R.E. "Mathematics of Reservoir Simulation ",Philadelphia (1983) 38-45

Fatt,I. and Maleki M.:"Detection and Estimation of Dead-End Pore Volume in Reservoir Rocks by Conventional Laboratory Tests", (1966) SPE 1441

Fourar, M., Konan, G., Fichen, C., Rosenberg, E., Egermann, P., and Lenormand., R. : "Tracer Tests for Various Carbonate Cores Using X-Ray CT",SCA Paper 2005-56, Toronto, Canada, 21-25 August 2005

Hagoort,J . :" The Response of Interwell Tracer Tests in Water-Out Reservoirs", (1982), SPE 11131

Hashemi, S. M., Kazemzadeh, E.-A. and Esfahani, M. R.: "Determination of Accessible Pore Volumes of a Porous Media during Miscible Displacement Using Tracer Analysis Technique", SCA Paper 2003-64, Pau, France, 2003

Jasti, J.K., Vaidya, R.N. and Fogler, H.S. ," Capacitance Effect in Porous Media," (1988), SPE 16707

Lønøy, A.: "Making Sense of Carbonate Pore Systems," manuscript in preparation, 2006.

Lucia, F.J.: "Petrophysical parameters estimated from visual descriptions of carbonate rocks: A field classification of carbonate pore space," Journal of Petroleum Tech., vol. 216, 221-224, 1983.

Perkins,T.K. and Johnston,O.C. "A Review of Diffusion and Dispersion in Porous Media," SPEJ (March 1963) 70-84

Salter, S.J. and Mohanty, K.K.: "Multiphase Flow in Porous Media: I. Macroscopic Observations and Modeling," paper SPE 11017 presented at the 1982 SPE Annual Technical Conference and Exhibition, New Orleans, Sept. 26-29. (1982)

Smith, L. and Schwartz, F.W.: "The Dispersive Flux in Transport Phenomena in Porous Media,"Adv. Water Recourses (Sept. 1983) 6, 169-74

A three Dimensional Chemical Flood Simulator (UTCHEM-9.82) Developed by the University of Texas at Austin, see manual July 2000

APPENDIX

Based on capacitance model given by Coats and Smith[3], a portion of pore volume can be divided into flowing and dead-end pore volumes:

$$PV_{CM} = PV_D + PV_f \quad \text{(A1)}$$

or

$$PV_D = (1-f)\cdot PV_{CM} \quad \text{(A2)}$$

$$PV_f = f \cdot PV_{CM} \quad \text{(A3)}$$

On the other hand, in the presence of inaccessible pore types, the total pore volume can be divided into an inaccessible pore volume and a portion detected by the capacitance model. This is shown in the following equation:

$$PV_T = PV_{CM} + PV_I \quad \text{(A4)}$$

By combining above equations, one can write:

$$PV_T = PV_D + PV_f + PV_I = (1-f)\cdot(PV_T - PV_I) + f\cdot(PV_T - PV_I) + PV_I \quad \text{(A5)}$$

Dividing above equation by Bulk Volume:

$$\phi_T = \phi_D + \phi_f + \phi_I = (1-f)\cdot(\phi_T - \phi_I) + f\cdot(\phi_T - \phi_I) + \phi_I \quad \text{(A6)}$$

Table 1–Summary of Basic Properties of Selected Core Materials and Experiments

Pore Class	Plug ID	Φt	K	Injection Tracer Rate	Recovery factor by Water flooding
		[fraction]	[mD]	[ml/min]	[fraction]
IC-UMa	F89	0.021	0.16	0.067	*
	F12	0.039	0.67	0.25	0.45
	F108	0.045	0.48	0.25	0.45
	F3	0.12	5..55	1	0.19
	F48	0.129	37.5	2	0.65
M-Mi	F25	0.15	0.15	0.167	0.42
	O-3	0.119	0.19	0.1	0.3
IC-PMi	O-10	0.115	0.86	0.5	0..2
	O-38	0.19	0.78	0.75	*
	O-39	0.221	0.71	0.5	0.58
IC-PMe	O-25	0.114	1.46	0.5	0.42
	O-9	0.186	13.7	1	0.58
	O-8	0.262	8.73	1	0.59
IC-UMi	O-35	0.18	0.18	0.17	0.34
Chalky-Micro (Cretaceous	OS-2	0.249	0.286	0.25	0.77
	OS-3	0.248	0.255	0.25	0.153
Vuggy	P1	0.263	2153	1.67	*
	P2	0.31	1504	1.67	0.59
	P3	0.289	1583	1.67	0.48
	P4	0.302	1335	1.67	0.43

Table2-Summary of Estimated Parameters to Analyze Tracer Injection and Dispersion Characteristics for Different Carbonate Pore Classes

Pore Class	Plug ID	α	(f)	Φf	ΦD	Φi
		[cm]	[fraction]	[fraction]	[fraction]	[fraction]
IC-UMa	F89	0.9	0.8	0.0118	0.0029	0.0063
	F12	0.9	0.65	0.0155	0.0083	0.0152
	F108	0.95	0.85	0.0344	0.0061	0.0045
	F3	0.69	0.6	0.054	0.036	0.03
	F48	0.61	1	0.123	0	0.0065
M-Mi	F25	0.3	0.9	0.135	0.015	0
	O-3	0.05	1	0.0764	0	0.043
IC-PMi	O-10	0.67	0.7	0.0664	0.029	0.020
	O-38	0.1	0.95	0.181	0.0095	0
	O-39	0.05	0.95	0.210	0.011	0
IC-PMe	O-25	0.6	0.98	0.105	0.0021	0.0068
	O-9	0.3	0.9	0.167	0.019	0
	O-8	0.07	0.9	0.236	0.026	0
IC-UMi	O-35	0.3	0.98	0.167	0.0034	0.0099
Chalky-Micro Cretaceous	OS-2	0.9	0.7	0.174	0.075	0
	OS-3	0.025	1	0.248	0	0
Vuggy	P1	0.1	1	0.171	0	0.092
	P2	0.03	0.8	0.201	0.05	0.059
	P3	0.03	0.8	0.187	0.047	0.055
	P4	0.025	0.8	0.106	0.027	0.170

*: Data are not available due to failure in measurement.

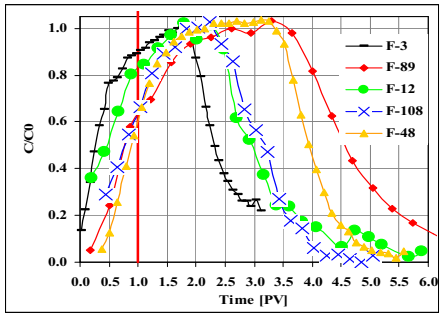

Figure 1. Tracer Profiles for Intercrystalline Uniform-Macro Pore Type

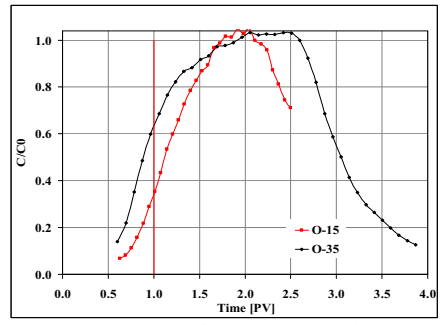

Figure 2. Tracer Profiles for Intercrystalline Uniform-Micro Pore Type

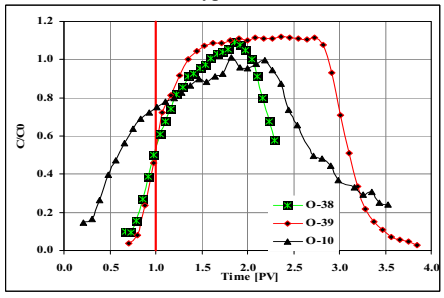

Figure3. Tracer Profiles for Intercrystalline Patchy-Micro Pore Type

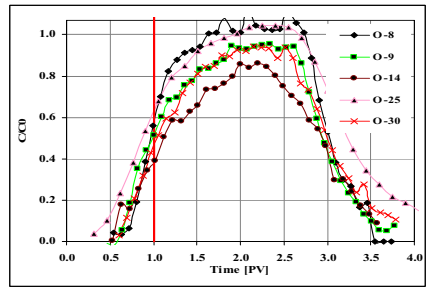

Figure 4. Tracer Profiles for Intercrystalline Patchy-Meso Pore Type

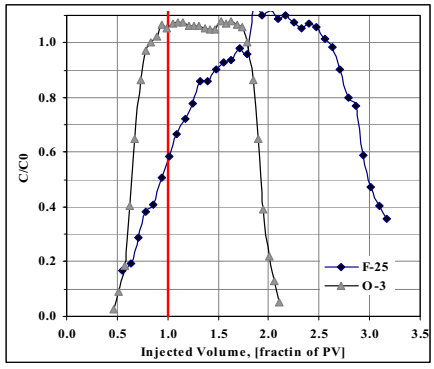

Figure 5. Tracer Profiles for Moldic- Micro Pore Type

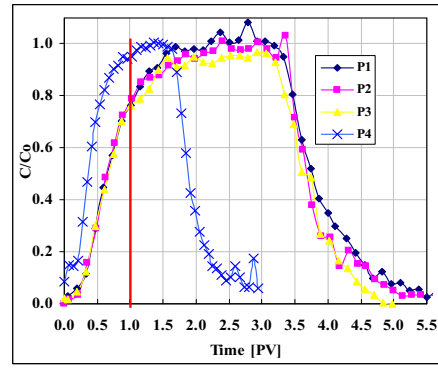

Figure 6. Tracer Profiles for Vuggy Pore Type

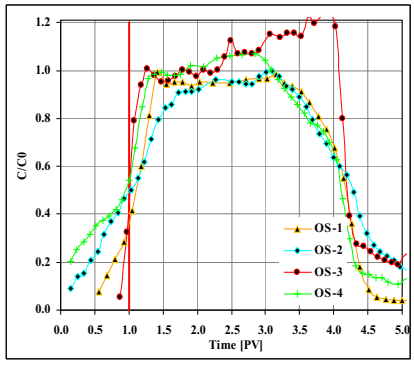

Figure 7. Tracer Profiles for Chalky-Micro Pore Type

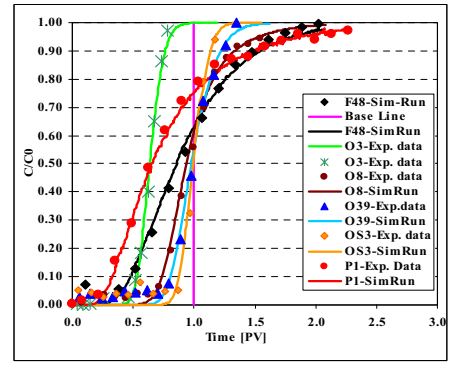

Figure 8. Examples of tracer response for cores where history match by the capacitance model were possible

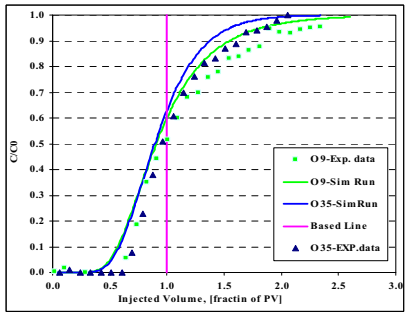

Figure 9. Descriptive Limits of Dispersion Characteristics by Capacitance Model due to Different Local Disperivity

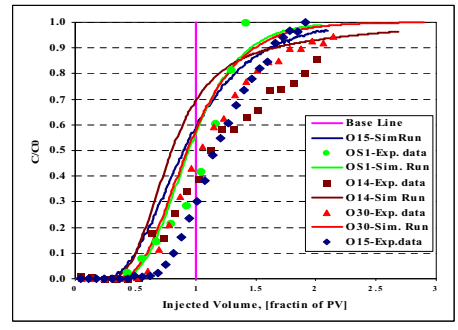

Figure 10. Examples of unsatisfactory match of multi-step dispersion (O-14)

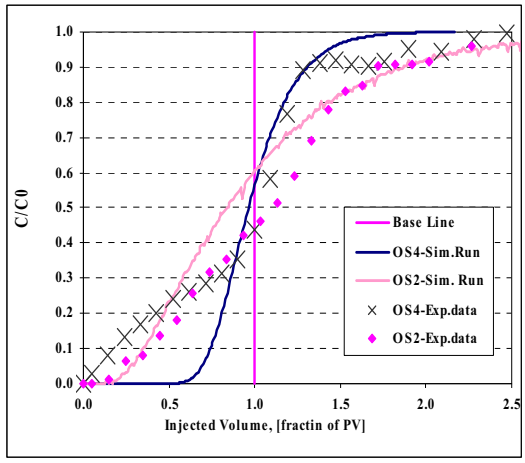

Figure 11. Experimental cases difficult to history match by the Capacitance Model

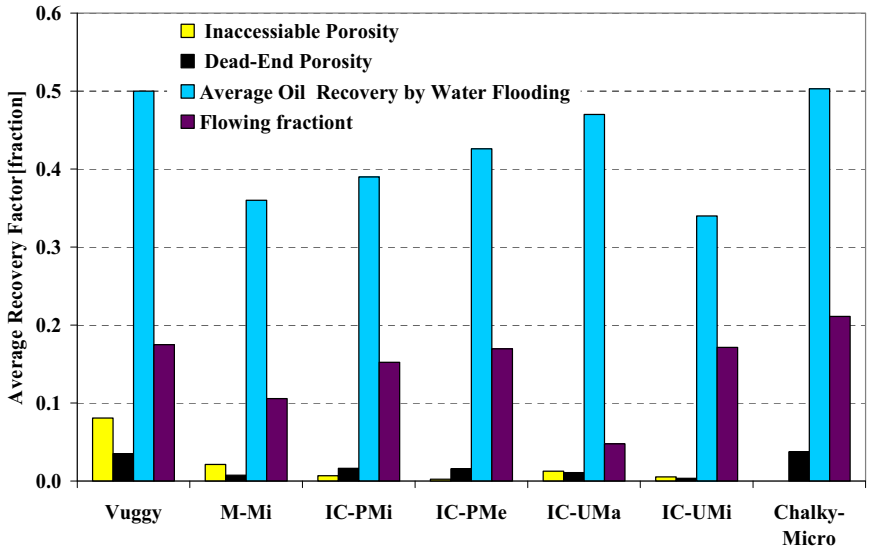

Figure 12. Average flowing fraction Porosity, Dead- End Pores Porosity, Inaccessible Porosity and Oil Recovery Factor by Water Flooding for Different Carbonate Pore Classes